SCIENTIFIC PUBLICATIONS OF THE STATE UNIVERSITY OF NOVI PAZAR
SERIES A: APPL. MATH. INFORM. AND MECH., Vol. 18, 1, 2026, 25–45

Calculation of Deflection of Rectangular Simply Supported Plates Using the Finite Difference Method. Interval Calculus

Emir Maslak, Nazim Manić, Ersin Gilić, Veis Šerifi, Timur Curić

Abstract: This paper presents the analysis of deflection of rectangular simply supported thin plates using the finite difference method. The governing fourth-order differential equation of plate bending is discretized and solved numerically within the Mathematica environment. The results are compared with those obtained using the analytical solution and finite element method (SAP2000), showing good agreement and confirming the accuracy of the applied approach. Additionally, interval calculus is introduced to account for uncertainties in input parameters such as load intensity, plate thickness, and material properties. This enables the evaluation of deflection within defined bounds, providing a more comprehensive insight into structural behavior. The study demonstrates that the combined use of the finite difference method and interval calculus represents an efficient and reliable tool for plate analysis.

Keywords and phrases: rectangular plate bending, finite difference method (FDM), interval calculus, numerical analysis, structural mechanics, plate theory, Kirchhoff plate model.

Manuscript received May 8, 2026; accepted July 25, 2026
Emir Maslak (ORCID 0009-0004-2189-4282) is with the State University of Novi Pazar, Vuka Karadžića 9, 36300 Novi Pazar, Serbia, emaslak@np.ac.rs
Nazim Manić (ORCID 0000-0001-8346-8255) is with the State University of Novi Pazar, Vuka Karadžića 9, 36300 Novi Pazar, Serbia, nmanic@np.ac.rs
Ersin Gilić (ORCID 0000-0002-0277-2675) is with the State University of Novi Pazar, Vuka Karadžića 9, 36300 Novi Pazar, Serbia, egilic@np.ac.rs
Veis Šerifi (ORCID 0000-0002-2639-9203) is with the State University of Novi Pazar, Vuka Karadžića 9, 36300 Novi Pazar, Serbia, serifiveis@np.ac.rs
Timur Curić (ORCID 0000-0001-5897-4279) is with the State University of Novi Pazar, Vuka Karadžića 9, 36300 Novi Pazar, Serbia, tcuric@np.ac.rs
https://doi.org/10.46793/SPSUNP2601.25M

1 Introduction

The application of plates as structural systems in civil engineering is extensive. They may be used as floor slabs, foundation slabs, retaining structures, bridge slabs, integral parts of complex hydraulic structures, and so on. According to the definition [1, 4, 7], plates are three-dimensional bodies bounded by two parallel planes, referred to as the bases, and by a cylindrical surface perpendicular to them, which represents the lateral boundary. The distance between the parallel planes, that is, the thickness of the plate, is small in comparison with the other linear dimensions of the plate. The middle plane of the plate is the plane that divides the thickness of the plate into two equal parts. According to their shape, plates may be rectangular, triangular, trapezoidal, circular, or irregularly shaped.

Modern analysis and design of engineering structures aims to prove, through the calculation process, the ability of the considered structure to carry the load assigned to it. This proof primarily refers to ensuring that the stress-strain state remains within permissible limits, while at the same time the economic factor must not be neglected.

The first step in the analysis consists of selecting a mathematical model that will represent the real structure in the best possible way and provide the possibility of calculating stresses and deformations. A mathematical model actually represents an idealization of the real structure, containing only those parameters that have the greatest influence on its real behavior. In the case of plates, idealization implies the introduction of certain assumptions that simplify the calculation, namely: the geometry of the plate and the method of support, the behavior of the material, and the type and method of load application.

It is clear that the most complex model would be the one that treats the plate as a three-dimensional model with nonlinear behavior. However, the calculation of such a model would be too extensive and therefore unsuitable for everyday engineering use. On the other hand, by introducing assumptions of linear elastic material behavior, small displacements, and small deformations, the analysis of the plate as a three-dimensional body can be reduced to solving the basic equations of the theory of elasticity.

Most of the proposed methods reduce the calculation of the plate to the calculation of a surface structure, taking into account the ratio of the plate thickness to the other dimensions. Depending on the ratio of the plate thickness to the shortest side of the plate, the following classification can be made:

(i) *very thin plates (membranes)* – surface structures without flexural stiffness, for which the ratio of thickness to the smallest dimension in the middle plane is approximately

$$h/b \leq (1/8 - 1/100),$$

(ii) *flexible plates* – plates that represent a combination of membrane and flexural stiffness,

(iii) *thin plates* – plates that are most widely used in civil engineering. The ratio of thickness to the shortest side is within the following limits:

$$(1/8 - 1/100) \leq h/b \leq (1/5 - 1/8),$$

(iv) *thick plates* – surface structures for which the ratio is:

$$h/b \geq (1/5 - 1/8).$$

For each type of plate, appropriate assumptions are introduced, which lead to the development of different theories dealing with the problem of plate bending.

As already stated, thin plates have the widest application in civil engineering, and therefore these plates are the subject of this paper. So far, a considerable number of useful engineering methods have been developed to describe the stress-strain state. Some of them are:

- *Navier's method*, used for the calculation of plates simply supported along their entire boundary,
- *Moriss-Levy's method*, used for the calculation of rectangular plates arbitrarily supported along their boundary.

With the development of computers, the problems that accompanied the analysis of plates using various numerical procedures have been overcome [2, 6]. Therefore, methods based on the finite difference method and the finite element method have now completely taken precedence.

2 Application of the Finite Difference Method in the Analysis of Thin Plates

The dominant stresses experienced by thin plates subjected to loads perpendicular to their plane are normal stresses caused by bending. The founder of the modern theory of plate bending is considered to be G. Kirchhoff (1824–1887). Based on his hypotheses [1, 4, 7] and assumptions, a differential equation of the plate was derived, which makes it possible to determine deflections at any point of the middle surface of the plate. This differential equation is, in fact, a fourth-order partial differential equation with respect to the unknown function $w(x,y)$ and has the form:

$$\nabla^4 w = \frac{\partial^4 w}{\partial x^4} + 2\frac{\partial^4 w}{\partial x^2 \partial y^2} + \frac{\partial^4 w}{\partial y^4} = \frac{q}{K} \tag{1}$$

where:

- q – distributed load expressed in $[kN/m^2]$,
- $K = \dfrac{Et^3}{12(1-\nu^2)}$ – flexural rigidity of the plate expressed in $[kNm]$,
- E – modulus of elasticity of the material (for concrete $E_b = 3.15 \cdot 10^7\, kN/m^2$),
- t – plate thickness $[m]$,
- ν – Poisson's ratio (for concrete $\nu = 0.20$).

A general solution of this differential equation does not exist. Depending on the boundary conditions, it is necessary to determine particular solutions. Only a limited number of problems can be solved in closed form suitable for everyday engineering practice.

In the case of a plate simply supported along its boundary, the boundary conditions are:

$$w = 0 \tag{2}$$

$$\frac{\partial^2 w}{\partial n^2} = 0, \tag{3}$$

where n denotes the normal to the edge in the direction of the x or y axis.

Introducing a new variable $u = \nabla^2 w$, the problem of solving equation (1) reduces to the successive solution of the Poisson equation in two iterations:

$$\nabla^2 u = \frac{q}{K}, \quad \text{with boundary conditions } u = 0 \text{ along all four edges,} \tag{4}$$

$$\nabla^2 w = u, \quad \text{with boundary conditions } w = 0 \text{ along all four edges.} \tag{5}$$

The application of the finite difference method to solving these differential equations consists of representing the given partial differential equations as a system of linear algebraic equations. The general form of the Poisson equation is:

$$\frac{\partial^2 \varphi}{\partial x^2} + \frac{\partial^2 \varphi}{\partial y^2} = \psi(x, y). \tag{6}$$

According to [3, 4], using central differences, the previous equation can be approximated as:

$$\frac{\varphi_{i-1,j} - 2\varphi_{i,j} + \varphi_{i+1,j}}{(\Delta x)^2} + \frac{\varphi_{i,j-1} - 2\varphi_{i,j} + \varphi_{i,j+1}}{(\Delta y)^2} = \psi_{i,j}. \tag{7}$$

The meaning of individual symbols is shown in Figure 1.

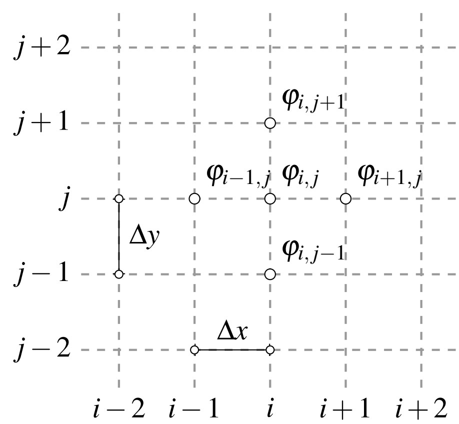

Figure 1: Finite difference grid and notation Δx i Δy.

Equation (5), expressed in terms of $\varphi_{i,j}$ in the general case, has the form:

$$\varphi_{i,j} = \frac{1}{2\left[(\Delta x)^2 + (\Delta y)^2\right]} \Big[\varphi_{i-1,j}(\Delta y)^2 + \varphi_{i+1,j}(\Delta y)^2 + \varphi_{i,j-1}(\Delta x)^2 + \\ + \varphi_{i,j+1}(\Delta x)^2 - \psi_{i,j}(\Delta x)^2(\Delta y)^2\Big]. \tag{8}$$

In the special case when $\Delta x = \Delta y$, equation (6) becomes:

$$\varphi_{i,j} = \frac{1}{4}\Big[\varphi_{i-1,j} + \varphi_{i+1,j} + \varphi_{i,j-1} + \varphi_{i,j+1} - \psi_{i,j}(\Delta x)^2\Big]. \tag{9}$$

In paper [5], this special case is analyzed, while the focus of this paper is the case where the steps of central differencing are different ($\Delta x \neq \Delta y$).

3 Determination of Deflection of a Rectangular Plate

Within the software system *Mathematica* [9], the deflection of a rectangular plate was calculated using the finite difference method. The plate is loaded and supported according to the layout shown in Figure 2. Two models were developed. One model was discretized such that the plate was divided into four elements along the x and y axes, while the second model divided the same plate into six elements along both axes. In addition, the plate deflection was also calculated using Navier's analytical solution, enabling a comparison between the numerical results obtained by the finite difference, finite element method and the analytical solution.

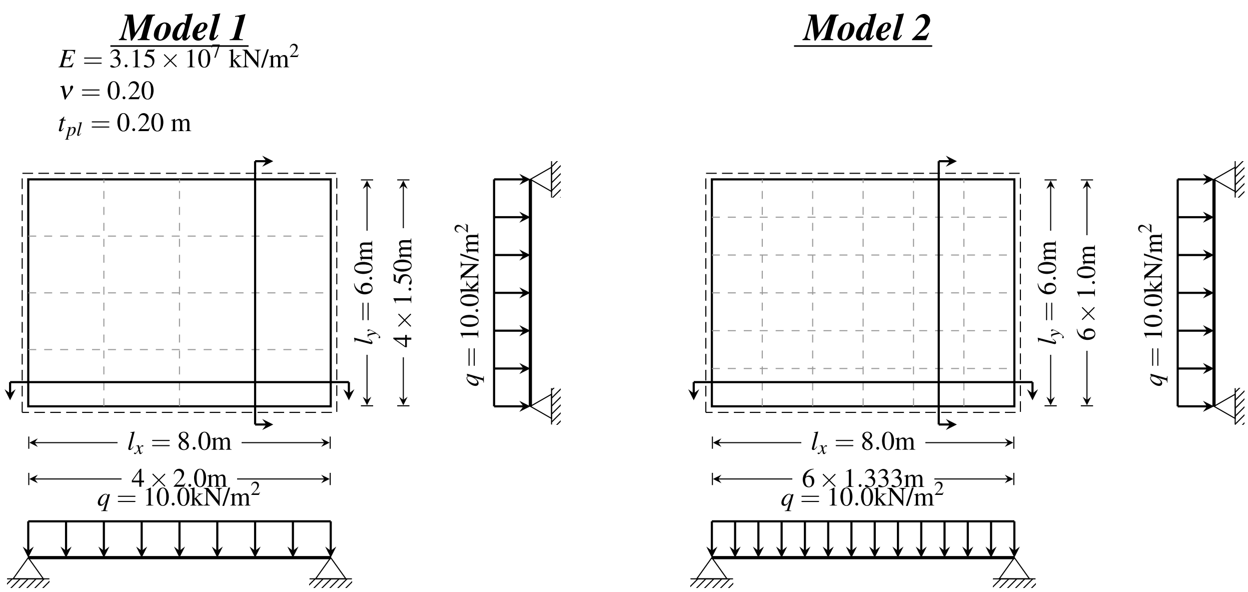

Figure 2: Plate models and discretization schemes

Two levels of discretization were used in order to observe the convergence of the solution to some extent. At the same time, the results obtained using the finite difference method were compared with the results obtained using the finite element method. The finite element analysis was performed using the software package SAP 2000 v.14.2 [8].

The designation of elements used in the program is given below:

Table 1: Meaning of symbols

Symbol	Description	Unit
n	Number of divisions along one side	–
n_{dis}	Number of discrete points along one side	–
i, j	Grid nodes	–
q	Load	kN/m^2
t	Plate thickness	m
ν	Poisson's ratio	–
l_x	Plate length in x direction	m
l_y	Plate length in y direction	m
Δx	Step size in x direction	m
Δy	Step size in y direction	m
E_b	Modulus of elasticity	kN/m^2
K_{pl}	Plate flexural rigidity	kNm
rhs	Ratio q/K_{pl} at each grid point	–
ϕ, ψ	Matrices of functions in the Poisson equation	–
u	Matrix of intermediate variable values	–
w	Deflection matrix at each point	m

Program implemented in Mathematica

Listing 1: Direct FDM solver for plate deflection calculation

```
ClearAll["Global`*"];

Print["***␣Direct␣FDM␣Solver␣for␣Plate␣Deflection␣***"];

n = 4; (* Number of divisions along one side: change as needed (e.
   g., 4, 6, 8...) *)
ndis = n + 1;

q = 10.0; (* Surface load q [kN/m^2] *)
t = 0.20; (* Plate thickness t [m] *)
nu = 0.20; (* Poisson's ratio *)
lx = 8.0; (* Plate length in the x-direction lx [m] *)
ly = 6.0; (* Plate length in the y-direction ly [m] *)
Eb = 31500000; (* Modulus of elasticity Eb [kN/m^2] *)

dx = lx/n;
```

```
dy = ly/n;

Kpl = (Eb*t^3)/(12*(1 - nu^2));
rhsVal = q/Kpl;

(* Function for mapping 2D grid index to 1D vector index *)
idx[i_, j_] := (i - 1)*ndis + j;

(* Constructing the FDM system matrix for the Laplace operator *)
matrixEntries = {};
rhsVec1 = Table[0., {ndis^2}];

Do[
  If[i == 1 || i == ndis || j == 1 || j == ndis,
    (* Boundary conditions: phi = 0 on the edges *)
    AppendTo[matrixEntries, {idx[i, j], idx[i, j]} -> 1.0];
    rhsVec1[[idx[i, j]]] = 0.0;,

    (* Interior nodes: 5-point FDM formula for Poisson's equation
        *)
    AppendTo[matrixEntries, {idx[i, j], idx[i, j]} -> -2.0*(1/dx^2
        + 1/dy^2)];
    AppendTo[matrixEntries, {idx[i, j], idx[i - 1, j]} -> 1/dx^2];
    AppendTo[matrixEntries, {idx[i, j], idx[i + 1, j]} -> 1/dx^2];
    AppendTo[matrixEntries, {idx[i, j], idx[i, j - 1]} -> 1/dy^2];
    AppendTo[matrixEntries, {idx[i, j], idx[i, j + 1]} -> 1/dy^2];

    rhsVec1[[idx[i, j]]] = -rhsVal;
  ],
  {i, 1, ndis}, {j, 1, ndis}
];

A = SparseArray[matrixEntries];

(* Step 1: Direct solution of the first Poisson equation Del^2(u)
    = -q/Kpl *)
uVec = LinearSolve[A, rhsVec1];
uMat = Partition[uVec, ndis];
```

```
(* Step 2: Preparing the right-hand side and solving the second
   Poisson equation Del^2(w) = -u *)
rhsVec2 = Table[0., {ndis^2}];
Do[
  If[!(i == 1 || i == ndis || j == 1 || j == ndis),
    rhsVec2[[idx[i, j]]] = -uMat[[i, j]];
  ],
  {i, 1, ndis}, {j, 1, ndis}
];

wVec = LinearSolve[A, rhsVec2];
wMat = Partition[wVec, ndis];

(* Output results *)
Print["Number␣of␣divisions␣n␣=␣", n];
Print["Step␣sizes:␣dx␣=␣", dx, "␣m,␣dy␣=␣", dy, "␣m"];
Print["Auxiliary␣matrix␣u␣=␣", MatrixForm[uMat]];
Print["Plate␣deflection␣matrix␣w␣=␣", MatrixForm[wMat]];
Print["Max␣deflection␣at␣center␣w_max␣=␣", Max[wMat], "␣m"];
```

Results obtained using Navier's analitycal solution

Based on Navier's analytical solution, the deflection of a simply supported rectangular plate subjected to a uniformly distributed load is determined by the following expression:

$$w(x,y) = \frac{16p}{k\pi^6} \sum_{m=1}^{\infty} \sum_{n=1}^{\infty} \frac{1}{mn\left(\frac{m^2}{a^2}+\frac{n^2}{b^2}\right)^2} \sin\left(\frac{m\pi x}{a}\right) \sin\left(\frac{n\pi y}{b}\right)$$

a) for $n = 4$:

$$w = \begin{bmatrix} 0 & 0 & 0 & 0 & 0 \\ 0 & 0.002077292 & 0.00281791 & 0.002077292 & 0 \\ 0 & 0.002885848 & 0.00392726 & 0.002885848 & 0 \\ 0 & 0.002077292 & 0.00281791 & 0.002077292 & 0 \\ 0 & 0 & 0 & 0 & 0 \end{bmatrix}$$

b) for $n = 6$:

$$w = \begin{bmatrix} 0 & 0 & 0 & 0 & 0 & 0 & 0 \\ 0 & 0.001080383 & 0.001776862 & 0.002010474 & 0.001776862 & 0.001080383 & 0 \\ 0 & 0.001827119 & 0.003021857 & 0.003424665 & 0.003021857 & 0.001827119 & 0 \\ 0 & 0.00208973 & 0.003463158 & 0.003927275 & 0.003463158 & 0.00208973 & 0 \\ 0 & 0.001827119 & 0.003021857 & 0.003424665 & 0.003021857 & 0.001827119 & 0 \\ 0 & 0.001080383 & 0.001776862 & 0.002010474 & 0.001776862 & 0.001080383 & 0 \\ 0 & 0 & 0 & 0 & 0 & 0 & 0 \end{bmatrix}$$

Results obtained using Mathematica

a) for $n = 4$:

$$w = \begin{bmatrix} 0 & 0 & 0 & 0 & 0 \\ 0 & 0.00205688 & 0.00285242 & 0.00206535 & 0 \\ 0 & 0.00278136 & 0.00386496 & 0.00279017 & 0 \\ 0 & 0.00206636 & 0.00286266 & 0.00207096 & 0 \\ 0 & 0 & 0 & 0 & 0 \end{bmatrix}$$

b) for $n = 6$:

$$w = \begin{bmatrix} 0 & 0 & 0 & 0 & 0 & 0 & 0 \\ 0 & 0.00105699 & 0.00178573 & 0.00204517 & 0.00179334 & 0.00106548 & 0 \\ 0 & 0.00173202 & 0.00294120 & 0.00337420 & 0.00295289 & 0.00174506 & 0 \\ 0 & 0.00196168 & 0.00333584 & 0.00382837 & 0.00334774 & 0.00197495 & 0 \\ 0 & 0.00174064 & 0.00295468 & 0.00338819 & 0.00296378 & 0.00175077 & 0 \\ 0 & 0.00106661 & 0.00180074 & 0.00200607 & 0.00180541 & 0.00100718 & 0 \\ 0 & 0 & 0 & 0 & 0 & 0 & 0 \end{bmatrix}$$

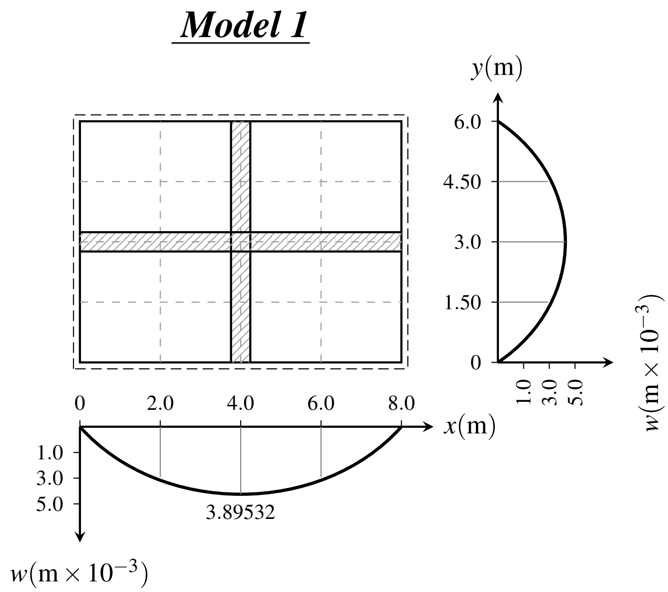

Figure 3: Deflection of the plate for $n = 4$ (Model 1)

Results obtained using the finite element method

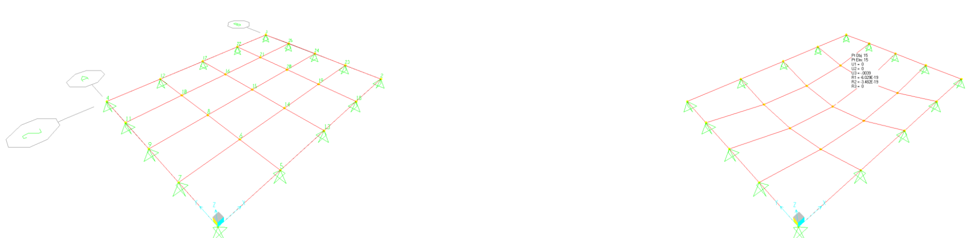

Figure 4: SAP 2000 model and plate deformation for Model 1 ($n = 4$)

Table 2: Finite element results for $n = 4$

Joint	**Output Case**	**Case Type**	U_3 **[m]**
1	Load Case 1	LinStatic	0.000000
2	Load Case 1	LinStatic	0.000000
3	Load Case 1	LinStatic	0.000000
4	Load Case 1	LinStatic	0.000000
5	Load Case 1	LinStatic	0.000000
6	Load Case 1	LinStatic	-0.002035
7	Load Case 1	LinStatic	0.000000
8	Load Case 1	LinStatic	-0.002842
9	Load Case 1	LinStatic	0.000000
10	Load Case 1	LinStatic	-0.002035
11	Load Case 1	LinStatic	0.000000
12	Load Case 1	LinStatic	0.000000
13	Load Case 1	LinStatic	0.000000
14	Load Case 1	LinStatic	-0.002793
15	Load Case 1	LinStatic	-0.003913
16	Load Case 1	LinStatic	-0.002793
17	Load Case 1	LinStatic	0.000000
18	Load Case 1	LinStatic	0.000000
19	Load Case 1	LinStatic	-0.002035
20	Load Case 1	LinStatic	-0.002842
21	Load Case 1	LinStatic	-0.002035
22	Load Case 1	LinStatic	0.000000
23	Load Case 1	LinStatic	0.000000
24	Load Case 1	LinStatic	0.000000
25	Load Case 1	LinStatic	0.000000

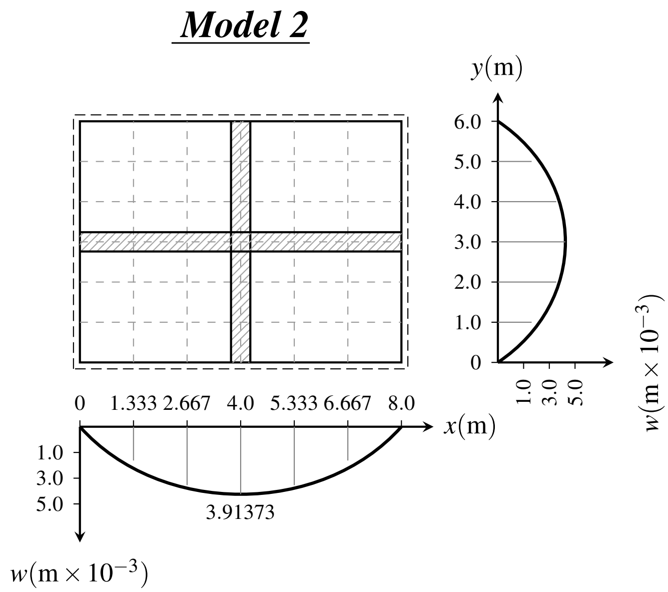

Figure 5: Deflection of the plate for $n = 6$ (Model 2)

Results obtained using the finite element method

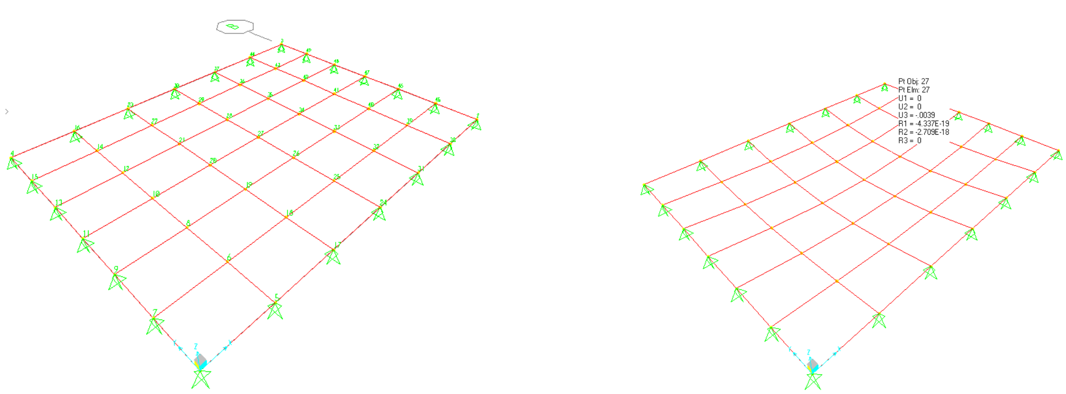

Figure 6: SAP 2000 model and plate deformation for Model 2 ($n = 6$)

Table 3: Finite element results for $n = 6$

Joint	**Output Case**	**Case Type**	U_3 **[m]**
1	Load Case 1	LinStatic	0.000000
2	Load Case 1	LinStatic	0.000000
3	Load Case 1	LinStatic	0.000000
4	Load Case 1	LinStatic	0.000000
5	Load Case 1	LinStatic	0.000000
6	Load Case 1	LinStatic	-0.001065
7	Load Case 1	LinStatic	0.000000
8	Load Case 1	LinStatic	-0.001807
9	Load Case 1	LinStatic	0.000000
10	Load Case 1	LinStatic	-0.002069
11	Load Case 1	LinStatic	0.000000
12	Load Case 1	LinStatic	-0.001807
13	Load Case 1	LinStatic	0.000000
14	Load Case 1	LinStatic	-0.001065
15	Load Case 1	LinStatic	0.000000
16	Load Case 1	LinStatic	0.000000
17	Load Case 1	LinStatic	0.000000
18	Load Case 1	LinStatic	-0.001764
19	Load Case 1	LinStatic	-0.003010
20	Load Case 1	LinStatic	-0.003453
21	Load Case 1	LinStatic	-0.003010

Table 4: Finite element results for $n = 6$ (continued)

Joint	**Output Case**	**Case Type**	U_3 **[m]**
22	Load Case 1	LinStatic	-0.001764
23	Load Case 1	LinStatic	0.000000
24	Load Case 1	LinStatic	0.000000
25	Load Case 1	LinStatic	-0.002000
26	Load Case 1	LinStatic	-0.003417
27	Load Case 1	LinStatic	-0.003923
28	Load Case 1	LinStatic	-0.003417
29	Load Case 1	LinStatic	-0.002000
30	Load Case 1	LinStatic	0.000000
31	Load Case 1	LinStatic	0.000000
32	Load Case 1	LinStatic	-0.001764
33	Load Case 1	LinStatic	-0.003010
34	Load Case 1	LinStatic	-0.003453
35	Load Case 1	LinStatic	-0.003010
36	Load Case 1	LinStatic	-0.001764
37	Load Case 1	LinStatic	0.000000
38	Load Case 1	LinStatic	0.000000
39	Load Case 1	LinStatic	-0.001065
40	Load Case 1	LinStatic	-0.001807
41	Load Case 1	LinStatic	-0.002069
42	Load Case 1	LinStatic	-0.001807
43	Load Case 1	LinStatic	-0.001065
44	Load Case 1	LinStatic	0.000000
45	Load Case 1	LinStatic	0.000000
46	Load Case 1	LinStatic	0.000000
47	Load Case 1	LinStatic	0.000000
48	Load Case 1	LinStatic	0.000000
49	Load Case 1	LinStatic	0.000000

Comparison of Results Obtained by the Analytical Solution, Finite Difference Method and Finite Element Method

Table 5 presents a comparison of the maximum deflection obtained using the analytical solution, the Finite Difference Method (FDM) and the Finite Element Method (FEM). The absolute error is computed as

$$\Delta_{\text{abs}} = \left| w_{\text{num}} - w_{\text{analytical}} \right|,$$

while the relative error is given by

$$\Delta_{\mathrm{rel}} = \frac{\Delta_{\mathrm{abs}}}{|w_{\mathrm{analytical}}|} \times 100\%.$$

Table 5: Comparison of analytical, FDM, and FEM results

n	**Method**	$w_{\max}$	Δ_{abs}	Δ_{rel} **(%)**
4	Analytical solution	0.00392728	0	0.0000
	FDM	0.00386496	0.00006232	1.5869
	FEM	0.00391300	0.00001428	0.3636
6	Analytical solution	0.00392728	0	0.0000
	FDM	0.00389938	0.00002790	0.7104
	FEM	0.00392300	0.00000428	0.1090

It can be observed that both numerical methods provide results that are in very good agreement with the analytical solution. As expected, increasing the number of discretization points from $n = 4$ to $n = 6$ reduces both the absolute and relative errors. Furthermore, the Finite Element Method exhibits smaller errors than the Finite Difference Method for both discretizations, indicating a higher level of accuracy for the considered problem.

4 Interval Calculus

Using the program presented in the previous section, it is possible to track the variation of plate deflection when certain parameters are defined within specified intervals.

Example 1. The input data used in this example are: $n = 4$, $q = 7.5 - 12.5\,\mathrm{kN/m^2}$, $t = 0.20\,\mathrm{m}$, $l_x = 8.0\,\mathrm{m}$, $l_y = 6.0\,\mathrm{m}$, $\nu = 0.20$, and $E = 3.15 \times 10^7\,\mathrm{kN/m^2}$. Interval calculus (IC) is introduced into the program in the following way:

```
q = Interval[{7.50, 12.50}];
```

Verification of the results at the interval bounds was performed using interval arithmetic in Wolfram Mathematica, yielding the following output:

```
Load q = Interval[{7.5, 12.5}] kN/m^2
Calculated Interval for max deflection
w_max = Interval[{0.00289872, 0.00483120}] m
```

```
Lower bound (q = 7.5)  : 0.00289872 m
Upper bound (q = 12.5) : 0.00483120 m
```

The matrix of results is:

$$w = \begin{bmatrix} 0. & 0. & 0. & 0. & 0. \\ 0. & [0.00156079, 0.00260131] & [0.00215980, 0.00359967] & [0.00156079, 0.00260131] & 0. \\ 0. & [0.00210589, 0.00350982] & [0.00292149, 0.00486915] & [0.00210589, 0.00350982] & 0. \\ 0. & [0.00156079, 0.00260131] & [0.00215980, 0.00359967] & [0.00156079, 0.00260131] & 0. \\ 0. & 0. & 0. & 0. & 0. \end{bmatrix}$$

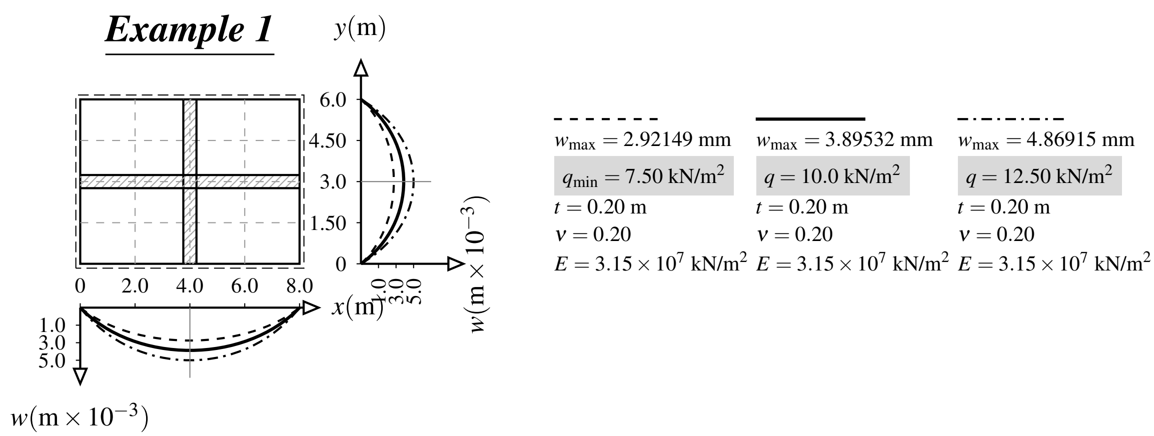

Figure 7: Deflection intervals for Example 1

In the same manner, verification was carried out for the remaining examples.

Example 2. The input data used in this example are: $n = 4$, $q = 7.5 - 12.5\,\text{kN/m}^2$, $t = 0.15 - 0.25\,\text{m}$, $l_x = 8.0\,\text{m}$, $l_y = 6.0\,\text{m}$, $\nu = 0.20$, and $E = 3.15 \times 10^7\,\text{kN/m}^2$. The matrix of results is:

$$w = \begin{bmatrix} 0. & 0. & 0. & 0. & 0. \\ 0. & [0.000799123, 0.00616607] & [0.00110582, 0.00853255] & [0.000799123, 0.00616607] & 0. \\ 0. & [0.00107822, 0.00831957] & [0.00149580, 0.01154170] & [0.00107822, 0.00831957] & 0. \\ 0. & [0.000799123, 0.00616607] & [0.00110582, 0.00853255] & [0.000799123, 0.00616607] & 0. \\ 0. & 0. & 0. & 0. & 0. \end{bmatrix}$$

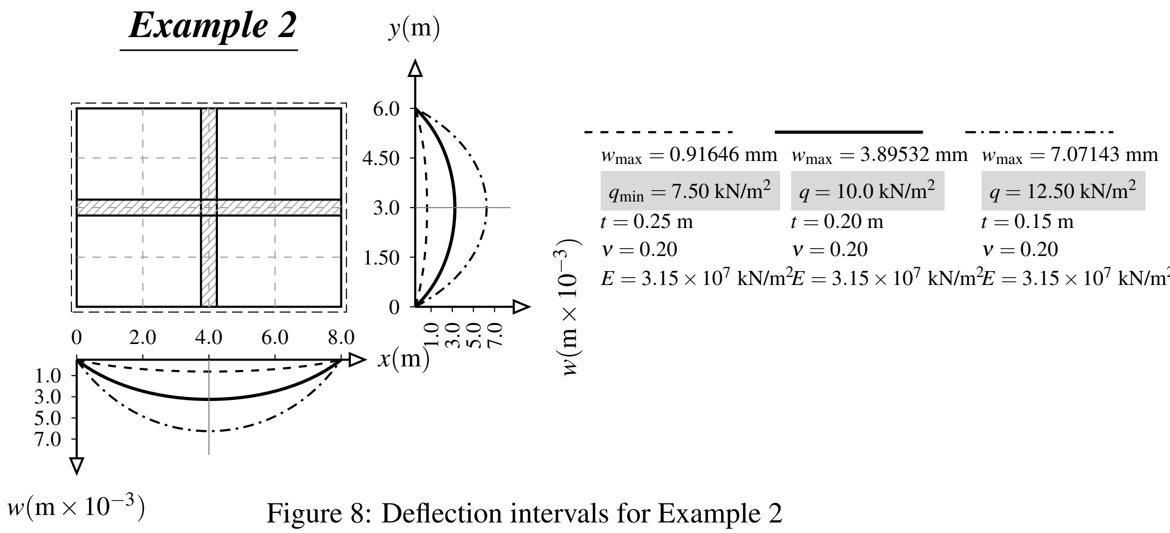

Figure 8: Deflection intervals for Example 2

Example 3. The input data used in this example are: $n = 4$, $q = 10.0\,\text{kN/m}^2$, $t = 0.20\,\text{m}$, $l_x = 7.75 - 8.25\,\text{m}$, $l_y = 6.0\,\text{m}$, $\nu = 0.20$, and $E = 3.15 \times 10^7\,\text{kN/m}^2$. The matrix of results is:

$$w = \begin{bmatrix} 0. & 0. & 0. & 0. & 0. \\ 0. & [0.00121825, 0.00395226] & [0.00166825, 0.00551647] & [0.00121825, 0.00395226] & 0. \\ 0. & [0.00162120, 0.00540776] & [0.00222759, 0.00756066] & [0.00162120, 0.00540777] & 0. \\ 0. & [0.00121825, 0.00395226] & [0.00166825, 0.00551648] & [0.00121825, 0.00395227] & 0. \\ 0. & 0. & 0. & 0. & 0. \end{bmatrix}$$

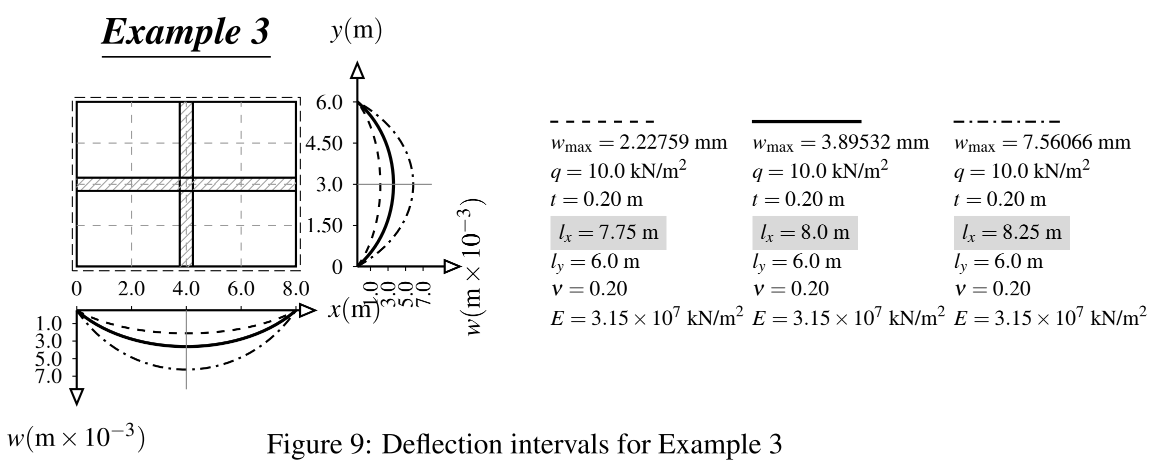

Figure 9: Deflection intervals for Example 3

Example 4. The input data used in this example are: $n = 4$, $q = 10.0\,\mathrm{kN/m^2}$, $t = 0.20\,\mathrm{m}$, $l_x = 8.0\,\mathrm{m}$, $l_y = 5.75 - 6.25\,\mathrm{m}$, $\nu = 0.20$, and $E = 3.15 \times 10^7\,\mathrm{kN/m^2}$.

The matrix of results is:

$$w = \begin{bmatrix} 0. & 0. & 0. & 0. & 0. \\ 0. & [0.00128393, 0.00355885] & [0.00176637, 0.00495213] & [0.00128393, 0.00355886] & 0. \\ 0. & [0.00170442, 0.00487076] & [0.00235220, 0.00679054] & [0.00170442, 0.00487076] & 0. \\ 0. & [0.00128393, 0.00355886] & [0.00176637, 0.00495214] & [0.00128393, 0.00355886] & 0. \\ 0. & 0. & 0. & 0. & 0. \end{bmatrix}$$

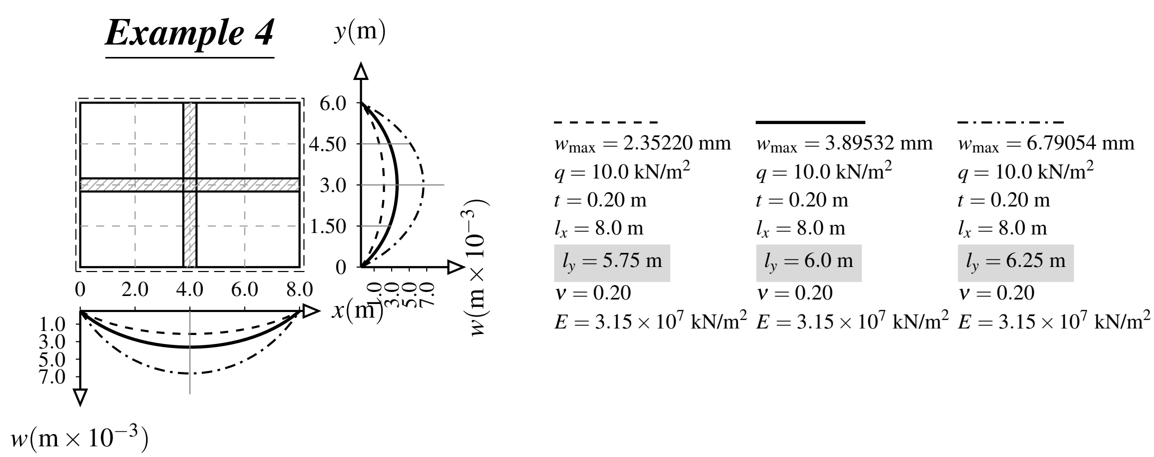

Figure 10: Deflection intervals for Example 4

Example 5. The input data used in this example are: $n = 4$, $q = 7.5 - 12.5\,\mathrm{kN/m^2}$, $t = 0.20\,\mathrm{m}$, $l_x = 8.0\,\mathrm{m}$, $l_y = 6.0\,\mathrm{m}$, $\nu = 0.20$, and $E = (2.85 - 3.40) \times 10^7\,\mathrm{kN/m^2}$.

The matrix of results is:

$$w = \begin{bmatrix} 0. & 0. & 0. & 0. & 0. \\ 0. & [0.00144602, 0.00287513] & [0.00200099, 0.00397858] & [0.00144602, 0.00287513] & 0. \\ 0. & [0.00195105, 0.00387927] & [0.00270667, 0.00538169] & [0.00195105, 0.00387927] & 0. \\ 0. & [0.00144602, 0.00287513] & [0.00200099, 0.00397858] & [0.00144602, 0.00287513] & 0. \\ 0. & 0. & 0. & 0. & 0. \end{bmatrix}$$

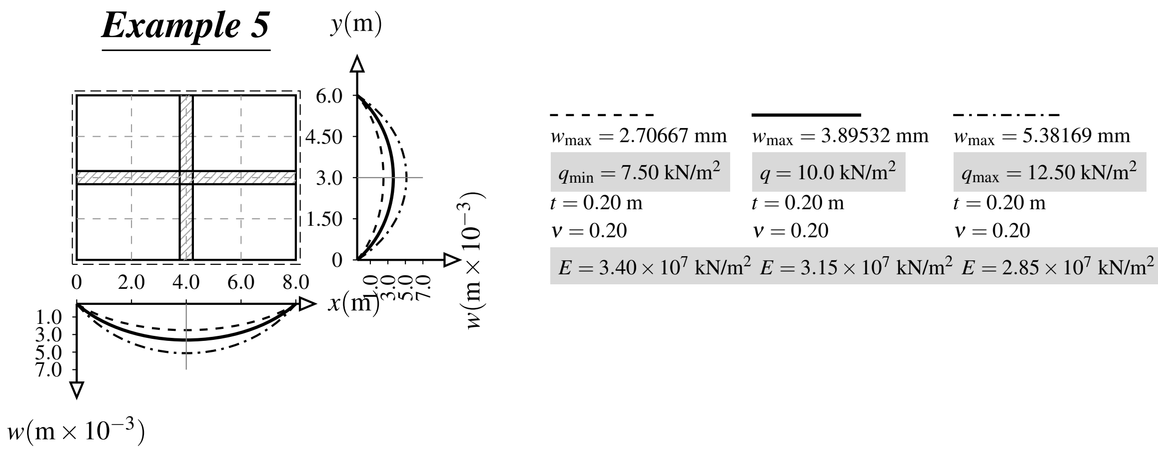

Figure 11: Deflection intervals for Example 5

5 Conclusions

This paper demonstrated the application of the Finite Difference Method (FDM) coupled with interval calculus for the deflection analysis of rectangular simply supported thin plates. The governing biharmonic differential equation was decomposed into two Poisson equations and solved using a direct sparse matrix formulation within Wolfram Mathematica. The quantitative findings confirm strong convergence toward Navier's analytical solution ($w_{\max}^{\text{analyt}} = 0.00392728$ m), where refining the discretization grid from $n = 4$ to $n = 6$ reduced the relative error of FDM from 1.5869% ($w_{\max} = 0.00386496$ m) down to 0.7104% ($w_{\max} = 0.00389938$ m), confirming theoretical $O(h^2)$ convergence. Furthermore, the Finite Element Method (SAP2000) exhibited relative errors of 0.3636% ($n = 4$) and 0.1090% ($n = 6$), showing excellent mutual agreement between both numerical approaches. Interval arithmetic effectively captured structural response bounds under input parameter uncertainties:

(i) a ±25% variation in surface load ($q \in [7.5, 12.5]$ kN/m^2) yielded a strictly linear maximum deflection range of $w_{\max} \in [0.00289872, 0.00483120]$ m;

(ii) plate thickness t demonstrated the highest sensitivity, where varying $t \in [0.15, 0.25]$ m led to a wide response bound of $w_{\max} \in [0.00149580, 0.01154170]$ m due to the cubic power dependence in flexural rigidity ($K_{pl} \propto t^3$); and

(iii) concrete elastic modulus variations ($E \in [2.85, 3.40] \times 10^7$ kN/m^2) combined with load intervals resulted in $w_{\max} \in [0.00270667, 0.00538169]$ m. By defining key input parameters as closed intervals, designers gain precise quantitative insight into the upper and lower bounds of structural responses. The combination of direct FDM solvers and interval arithmetic provides an efficient, computationally robust, and accurate tool for structural design under uncertain engineering environments.

References

[1] Ć. B. DOLIĆANIN, V. B. NIKOLIĆ, D. Ć. DOLIĆANIN, *Application of Finite Difference Method to Study of the Phenomenon in the Theory of Thin Plates*, Scientific Publications of the State University of Novi Pazar, Ser. A: Appl. Math. Inform. and Mech., 2(1) (2010), 29–43.

[2] Đ. R. ĐORĐEVIĆ, D. PETKOVIĆ, D. ŽIVKOVIĆ, *The Appliance of Interval Calculus in Estimation of Plate Deflection by Solving Poisson's Bisquared Partial Differential Equation*, Facta Universitatis, Series: Architecture and Civil Engineering, 6(2) (2008), 207–220. https://doi.org/10.2298/FUACE0802207D

[3] J. D. FAIRES, R. L. BURDEN, *Numerical Methods*, Third Edition, Brooks/Cole, 2002.

[4] N. HAJDIN, *Teorija površinskih nosača: Ploče napregnute na savijanje i ploče napregnute u svojoj ravni*, Drugo izdanje, Naučna Knjiga, Građevinski fakultet, Beograd, 1989.

[5] R. J. LEVEQUE, *Finite Difference Methods for Differential Equations*, University of Washington, 2005.

[6] G. V. MILOVANOVIĆ, Đ. R. ĐORĐEVIĆ, *Numerical Methods in Computational Engineering*, Faculty of Civil Engineering and Architecture, University of Niš, 2007.

[7] R. SALATIĆ, *Teorija površinskih nosača – Predavanja*, Građevinski fakultet, Univerzitet u Beogradu, 1991.

[8] SAP 2000, *Computer Structural Analysis Program: Analysis Reference*, Computers and Structures Inc., Berkeley, California, USA, 1996.

[9] WOLFRAM RESEARCH, *Wolfram Mathematica*, Available at: `https://www.wolfram.com`